

Organic & Biomolecular Chemistry

Accepted Manuscript



This is an *Accepted Manuscript*, which has been through the Royal Society of Chemistry peer review process and has been accepted for publication.

Accepted Manuscripts are published online shortly after acceptance, before technical editing, formatting and proof reading. Using this free service, authors can make their results available to the community, in citable form, before we publish the edited article. We will replace this *Accepted Manuscript* with the edited and formatted *Advance Article* as soon as it is available.

You can find more information about *Accepted Manuscripts* in the [Information for Authors](#).

Please note that technical editing may introduce minor changes to the text and/or graphics, which may alter content. The journal's standard [Terms & Conditions](#) and the [Ethical guidelines](#) still apply. In no event shall the Royal Society of Chemistry be held responsible for any errors or omissions in this *Accepted Manuscript* or any consequences arising from the use of any information it contains.

The design, synthesis and biological evaluation of novel thiamin diphosphate analog inhibitors against pyruvate dehydrogenase multienzyme complex E1 from *Escherichia coli*

Lingling Feng,^a Junbo He,^{a, b} Haifeng He,^a Lulu Zhao,^a Lingfu Deng,^c Li Zhang,^a Lin Zhang,^a Yanliang Ren,^a Jian Wan,*^a and Hongwu He*^a

^aKey Laboratory of Pesticide & Chemical Biology (CCNU), Ministry of Education; College of Chemistry, Central China Normal University, Wuhan 430079, China.

^bCollege of Food Science and Engineering, Wuhan Polytechnic University, Wuhan 430023, China

^cCollege of life science, Central China Normal University, Wuhan 430079, China.

Key words: microbicide; molecular docking; pyruvate dehydrogenase multienzyme complex E1; site-directed mutagenesis; thiamin diphosphate analog inhibitor.

*** Correspondence author:**

Jian Wan Tel & Fax: 86-27-67862022 E-mail: jianwan@mail.ccnu.edu.cn,

Hongwu He Tel & Fax: 86-27-67867960 E-mail: he1208@mail.ccnu.edu.cn

Abstract

Pyruvate dehydrogenase multienzyme complex E1 (PDHc E1) is a potential target enzyme for finding inhibitors to combat microbial disease. In this study, we designed and synthesized a series of novel thiamin diphosphate (ThDP) analogs with triazole ring and oxime ether moieties as potential inhibitors of PDHc E1. Their inhibitory activities against PDHc E1 were further examined *in vitro* and *in vivo*. Most of the tested compounds exhibited moderate inhibitory activities against PDHc E1 (IC_{50} = 6.1 - 75.5 μ M). The potent inhibitors 4g, 4h and 4j had strong inhibitory activities, with IC_{50} values of 6.7, 6.9 and 6.1 μ M against PDHc E1 *in vitro* and with inhibition rate 35%, 50% and 33% at $100\mu\text{g mL}^{-1}$ against *Gibberella zeae in vivo*, respectively. The binding mode of this compound (4j) to PDHc E1 was analyzed by a molecular docking method. Furthermore, the possible interaction of the important residues of PDHc E1 with compound 4j was examined by site-directed mutagenesis, enzymatic assays and spectral fluorescence studies. The theoretical and experimental results agree well. This suggests that compound 4j could be used as a lead compound for further optimization and may have potential as a new microbicide.

1. Introduction

Pathogenic microbe such as *Botrytis cinerea*, *Gibberella zeae*, *Rhizoctonia solani*, and *Escherichia coli* are hazardous to modern agriculture and human health.^{1, 2} Although there are microbicide (carbendazim, pyrimethanil, and ciprofloxacin) used for these pathogenic microbial infections, the severe side effects and toxicity of these microbicides and the increasing resistance to the microbicide have been recorded worldwide and are important factors resulting in treatment failure.^{3, 4} Therefore, it is of general interest to develop new and efficient microbicide with novel structures or modes of action or even new drug targets to overcome microbial disease.

The pyruvate dehydrogenase multienzyme complex (PDHc) plays a vital role in cellular metabolism and catalyzes the oxidative decarboxylation of pyruvate and the subsequent acetylation of coenzyme A (CoA) to acetyl-CoA during the tricarboxylic acid metabolic pathway.⁵ PDHc contains three enzymatic components: pyruvate dehydrogenase (E1), dihydrolipoamide acetyltransferase (E2), and dihydrolipoamide dehydrogenase (E3).⁵ The pyruvate dehydrogenase (PDHc E1) portion has two active sites: the substrate binding site and the cofactor thiamin diphosphate (ThDP) binding site. The PDHc E1 catalyzes the first step of this complex process and is an important target enzyme for finding inhibitors.⁶

Much effort has been made to design and synthesize the inhibitors of PDHc E1 including the PDHc E1 substrate analogs and cofactor ThDP analogs (**Fig. 1**).⁷⁻¹² These ThDP analog inhibitors, such as thiamin thiazolone diphosphate (ThTDP) and thiamine thiothiazolone diphosphate (ThTTDP), can block the formation of a covalent adduct between the substrate pyruvate and cofactor ThDP through the C2 atom of the thiazolium ring in the reaction pathway for PDHc E1.¹¹⁻¹⁵ These ThDP analog inhibitors exhibit significantly stronger binding affinities for PDHc E1 than ThDP and have received increasing attention.¹³ However, due to their complex structure with highly charged pyrophosphate groups, these ThDP analogs exhibit no potential utility and display poor bioavailability.¹¹⁻¹⁵

The crystal structures of the PDHc E1/ThDP complex and the PDHc E1/inhibitor (ThTDP) complex from *E.coli* (PDB ID: 1L8A and 1RP7) have been determined.^{14, 15} These structures reveal the detailed

characterization of the active site of PDHc E1, and provide a solid basis for understanding structure and mechanism. They enable structure-based design of novel inhibitors against PDHc E1. In our laboratory, we have carried out a systematic study for the design and synthesis of inhibitors against PDHc E1 as herbicide (HW02) (**Fig. 1**).¹⁶ The mechanism was predicted with theory.^{17, 18} The herbicide HW02 was found to be effective inhibitor against PDHc E1. Docking studies were employed to shed light on the binding mode of the interactions.

The triazole ring moiety can be tuned to form powerful pharmacophores and plays an important role in bio-conjugation, and the triazole ring moiety is a useful building block in organic synthesis because of its wide range of biological activity.^{19, 20} The oxime ether derivatives have attracted recent attention in medicinal chemistry research due to their excellent antibacterial or antifungal or antimicrobial activities.²¹⁻²⁴ These results encouraged us to explore and design novel ThDP analog inhibitors against PDHc E1 possessing microbicide activity by introducing the triazole ring and oxime ether moieties. Here we report the design and synthesis of a series of new compounds incorporating the active triazole ring and oxime ether pharmacophores and evaluate their inhibitory activities against PDHc E1 from *E. coli*. Furthermore, the mode of interaction of the important residues of PDHc E1 with the hit compound was examined by molecular docking experiments, site-directed mutagenesis, and enzymatic assays.

2. Results and discussion

2.1 Design and synthesis of the new ThDP analog inhibitors (4a - 4l)

The crystal structures of the PDHc E1/ThDP complex and the PDHc E1/inhibitor (ThTDP) complex from *E. coli* (PDB ID: 1L8A and 1RP7) provides detailed characterization of the active site of PDHc E1 and facilitates our design of new ThDP inhibitors targeted to the active site of PDHc E1.^{14, 15} The ThDP consists of three parts: diphosphate group, aminopyrimidine, and thiazolium moiety, which are bound in a “V” conformation involving the N-terminal and middle domains of PDHc E1.¹⁴ Due to the excellent antibacterial, antifungal, and antimicrobial activities of the oxime ether as well as the high charge of the pyrophosphate group, we expected that the oxime ether moiety of the new inhibitor

(shown in red) can substitute for the diphosphate group and avoid the high charge of the pyrophosphate group (**Fig. 2**).^{13, 21-24}

The PDHc E1 is initiated by the formation of a covalent adduct between the substrate and the cofactor through the C2 atom of the thiazolium ring in the reaction pathway of PDHc E1.^{14, 15} The triazole ring moiety has a surprisingly stable structure with three adjacent nitrogen atoms and has a wide range of biological activity and also plays an important role in bio-conjugation.^{19, 20} We expected that the new inhibitor with the triazole ring moieties could block this site by replacing the proton on C2 with a nitrogen atom in triazole ring moieties (shown in blue) of the novel ThDP analog inhibitors (**Fig. 2**). The aminopyrimidine ring was maintained for the proper orientation of the newly designed inhibitors because the aminopyrimidine ring hydrogen bonds to the active site of PDHc E1, which is partly responsible for the proper orientation of the cofactor ThDP.¹⁴ The structure of the new inhibitor is shown as **Fig. 2**.

The synthetic route used for compounds **4a - 4l** is depicted in **Scheme 1**. Intermediates **1a - 1l** were synthesized using various substituted benzaldehydes or acetophenones and react with hydroxylamine hydrochloride in the presence of potassium carbonate.²⁵ Compounds **1a - 1l** were then converted into intermediates **2a - 2l** in the presence of 3-bromopropyne using NaOH as base.²⁶ The 5-azidomethyl-2-methylpyrimidine-4-ylamine **3** was readily prepared from thiamine hydrochloride (ThDP) according to literature reports.²⁷ Finally, the Cu-catalyzed 1, 3-dipolar cycloaddition reaction was used to assemble the oxime ether **4a - 4l** employing copper (I) iodide- triethylamine (TEA) in THF.²⁸ The oxime-ether compounds are stable in the solid and solution states. The final compounds **4a - 4l** were purified by recrystallization from dimethyl formamide-water and characterized by ¹H NMR, ¹³C NMR, mass spectrometry (MS), and elemental analysis.

2.2 Inhibitory activities of the new ThDP analog inhibitors (**4a - 4l**) against *E.coli* PDHc E1

The synthesized ThDP analog inhibitors (**4a - 4l**) were evaluated for their inhibitory activities (half maximal inhibitory concentration, IC₅₀) against *E.coli* PDHc E1 (**Table 1**). The compounds had moderate inhibitory activities (IC₅₀ = 6.1 - 75.5 μM) except for the compound **4b** (IC₅₀ > 100μM). Compound **4h**, **4i** and **4j** proved to be the potent inhibitor with IC₅₀ values of 6.7, 6.9 and 6.1μM

against PDHc E1 *in vitro* respectively. Therefore, the inhibitory rates against *Gibberella zeae in vivo* of compound **4h**, **4i** and **4j** were further examined. By biological evaluation, compound **4h**, **4i** and **4j** had inhibition rates 35%, 50% and 33% at 100 $\mu\text{g. mL}^{-1}$ against *Gibberella zeae in vivo*, respectively.

To explore the structure-activity relationships (SAR) we first changed the R¹ group by using H (compounds **4a** - **4f**) or CH₃ (compounds **4g** - **4l**). The modifications are focused on R¹, in which the oxime ether group locates in the active site of PDHc E1. The inhibitory potencies of the two groups were obviously different (**Table 1**). In all categories, the inhibitory activities of the compounds with which the R¹ group is substituted with methyl (R¹ = CH₃, compounds **4g** - **4l**) are higher than those with H (R¹ = H, compounds **4a** - **4f**). Subsequently, we fixed the R¹ group as methyl (R¹ = CH₃) and changed R² group. The para-substituted analogs R¹ = CH₃, R² = 4-Cl (compound **4i**) showed higher inhibitory activity (IC₅₀ 6.9 \pm 1.2 μM) as compared to ortho- or meta-substituted compounds (R₁ = CH₃, R₂ = 2-Cl (compound **4l**) or R₁ = CH₃, R₂ = 3-Cl (compound **4g**). This implies that para-substitution is important for the inhibitory activity of the new oxime ether derivatives. In this case, compounds with electron-withdrawing groups on the aromatic ring (compounds **4h**, **4i**, and **4j**) were more effective than those bearing electron-donating methoxy (compound **4k**).

2.3 Analyses of the interaction between the novel ThDP analog inhibitors and PDHc E1

Compound **4j** was selected for the study of the interaction mode of the novel ThDP analog inhibitors (**4a** - **4l**) with *E.coli* PDHc E1 because it exhibited the highest inhibitory activity (IC₅₀ 6.1 \pm 0.5 μM) against PDHc E1.

We performed molecular docking studies via site-directed mutagenesis, enzymatic assays, and fluorescence spectral analyses. As shown in **Fig. 3**, compound **4j** is bound to the active site of PDHc E1, which has the 'V' conformation.^{14, 15}

The aminopyrimidine ring of compound **4j** has similar interactions with the amino acid residues to ThDP or ThTDP in the 'V' conformation, i.e., there is strong π - π stacking with the side chain ring of F602, and there are hydrogen bonds interactions between the main chain oxygen of V192, and two key hydrogen atoms. These hydrogen bonds are between the N₁' of the pyrimidine ring and the side chain of E571, and N₂' of the pyrimidine ring with the side chain of M194. The hydrogen bonds and

the π - π stacking are responsible for the proper orientation of aminopyrimidine of the compounds to the active site of PDHc E1 (**Fig. 3**). Packing contacts with M194 are important in stabilizing the cofactor ThDP construction as shown in the corresponding I415 in PDC.²⁹ In line with our docking prediction, the IC₅₀ values of compound **4j** against M194A mutant (69.9 μ M) and V192A (57.8 μ M) were about 11.5-fold and 9.5-fold higher than that against the wild-type enzyme (6.1 μ M), respectively (**Fig. 4**). The results also revealed that compound **4j** has stronger hydrogen bonding interaction with the residues M194 (26.8-fold) and V192 (29-fold) than ThDP based on the lower IC₅₀ values for compound **4j** with M194A (69.9 μ M) and V192A (57.8 μ M). The K_d for ThDP with M194A is 2.6 μ M and 2.0 μ M for V192A. These results suggested that the hydrogen bonding interaction between compound **4j** and M194 or V192 is an important pharmacophoric feature.

In the middle of the 'V' conformation, the thiazolium ring of ThDP mainly interacts with the residue I569 and D521.¹⁵ During turnover, the C2 of the thiazolium ring reacts with pyruvate to form 2- α -lactyl ThDP, which in turn undergoes decarboxylation to the 2- α -hydroxyethylidene-ThDP—an intermediate in the PDHc E1 reaction pathway. The Y177 might interact with the reaction intermediate.¹² In the vicinity of the C2 of the thiazolium ring, there is a cluster of histidine residues, including H640, H142, and H106, which likely attract and orient the negatively charged substrate pyruvate. Residue H640 can form hydrogen bonds with the pyruvate acid and partly responsible for its proper orientation.^{14, 15} In compound **4j**, we substituted the thiazolium ring with the triazole ring, which forms two hydrogen bonds with residues Y177 and H640, respectively.

In our model docking study, compound **4j** exhibits a strong interaction with residues Y177 and H640. Site-directed mutagenesis and enzymatic assays showed that the IC₅₀ values of compound **4j** against the Y177A (150.7 \pm 3.8 μ M) and H640A (53.9 \pm 2.7 μ M) mutants are about 39.5-fold and 8.8 higher than that against the wild type enzyme (6.1 μ M) (**Fig. 4**). This suggests that the hydrogen bonds interaction between compound **4j** and Y177 or H640 is also an important pharmacophoric feature.

Our docking results also showed that the oxime ether group attached to the aromatic ring in compound **4l** not only forms hydrogen bonds with H106, H142, and N260, but also coordinates with the metal ion (Mg²⁺) in the active site. Site-directed mutagenesis and enzymatic assays showed that

the IC_{50} values of compound **4j** against the H106 ($52.7 \pm 2.8 \mu\text{M}$) and H142A ($32.1 \pm 1.4 \mu\text{M}$) mutants are about 8.6 and 5.3-fold higher than that against the wild-type enzyme ($6.1 \mu\text{M}$) (**Fig. 4**), suggesting that H106 and H142 play important roles in the binding of compound **4j**. However, compound **4j** has stronger interactions with H106 (66.7-fold) and similar interaction with H142 (0.8-fold) than ThDP according to the IC_{50} values for compound **4j** with H106A ($52.7 \pm 2.8 \mu\text{M}$) and H142A ($32.1 \pm 1.4 \mu\text{M}$) compared to the K_d for ThDP with H106A ($0.8 \pm 0.02 \mu\text{M}$) and H142A ($38.1 \pm 1.7 \mu\text{M}$), respectively. These results imply that H106 is one of the most important residues affecting the binding of compound **4j** to the active site of PDHc E1.

It is impossible to understand the theoretically predicted binding model directly through the enzymatic assay of N260A mutant because the mutant exhibits much less enzymatic activity. To further validate the interaction between compound **4j** and N260A, the binding constant (K_b) values of the N260A were investigated using fluorescence spectral data. The K_b value of N260A (149 M^{-1}) is over 14-fold lower than the K_b value of the wild type enzyme (2108 M^{-1}) (**Fig. 5**), suggesting that there is stronger interaction between N260 and compound **4j** than with wild-type enzyme. These results further validate and explain the binding-mode between the inhibitors and active site of PDHc E1.

3. Conclusion

In this study we designed and synthesized a series of novel ThDP analogs as potential inhibitors of PDHc E1. Most of the compounds exhibited moderate inhibitory activities ($IC_{50} = 6.1 - 75.5 \mu\text{M}$). Compounds **4h**, **4i**, and **4j** were identified as the potent inhibitors with IC_{50} values of 6.7, 6.9 and 6.1 μM against PDHc E1 *in vitro*, and with inhibition rate 35%, 50% and 33% at $100 \mu\text{g mL}^{-1}$ against *Gibberella zeae in vivo*, respectively. The possible interaction of the important residues of PDHc E1 with compound **4j** binding to PDHc E1 was analyzed by molecular docking methods, site-directed mutagenesis, enzymatic assays, and fluorescence spectral analyses. The theoretical and experimental results agree well, indicating that compound **4j** could be used as a lead compound for further optimization and may have potential as a new microbicide.

4. Experimental procedures

4.1 General procedures

Melting points (mp) were measured on an electrothermal melting point apparatus and were uncorrected. The ^1H NMR spectra were recorded in DMSO- d_6 on a Varian Mercury-Plus 600 spectrometer at 600 MHz, the ^{13}C NMR spectra were recorded in DMSO- d_6 on a Varian Mercury-Plus 400 spectrometer at 100 MHz and chemical shifts were recorded in parts per million (ppm) with TMS as the internal reference. Mass spectra (MS) were obtained on a Trace MS 2000 instrument. Elemental analyses (EA) were measured on a Vario ELIII CHNSO elemental analyzer. Unless otherwise noted, reagents were purchased from commercial suppliers and used without further purification. Intermediate **3** was synthesized according to existing methods.²⁷

4.1.1 General procedure for preparation of compounds **1a - 1l**

A solution of benzaldehydes or acetophenones (10 mmol), hydroxylamine hydrochloride (1.39 g, 20 mmol), and anhydrous potassium carbonate (2.8 g, 20 mmol) in ethanol (10 mL) was heated under reflux until the reaction was complete based on TLC monitoring. The solvent was then removed under reduced pressure. The residue was dissolved in water (10 mL), and the solid was filtered and recrystallized from ethanol to yield compounds **1a - 1l**, which were used directly for the next step.

4.1.2 General procedure for preparation of compounds **2a - 2l**

We added sodium hydroxide (0.2 g, 5 mmol) to a solution of **1a - 1l** (5 mmol) and 3-bromopropyne (0.6 g, 5 mmol) in dry acetonitrile (20 mL). The mixture was heated under reflux until completion (as monitored via TLC), and the solvent was removed under reduced pressure. The residue was dissolved in ethyl acetate (50 mL) and washed with 0.1 M HCl, and brine and then dried and concentrated. The crude product was recrystallized with acetone to give the pure compounds **2a - 2l**, which were used directly for the next step.

4.1.3 General procedure for preparation of compounds **4a - 4l**

We added CuI (0.04 g, 2 mmol) to a stirred solution of 5-azidomethyl-2-methylpyrimidine-4-ylamine **3** (0.33 g, 2 mmol) and **2a - 2l** (2 mmol) in THF (10 mL) followed by Et_3N (0.4 g, 4 mmol). After overnight stirring at room temperature and the reaction mixture was poured into water (50 mL), and

the precipitate was collected by filtration and dried under atmospheric pressure. Recrystallization with DMF/H₂O afforded compounds **4a** - **4l**.

4.1.3.1 Benzaldehyde *O*-((1-((4-amino-2-methylpyrimidin-5-yl) methyl)-1H-1, 2, 3-triazol-4-yl) methyl) oxime (4a**)**

Yellow solid; 0.59g; Yield 92%; m.p. 170 - 172°C; ¹H NMR (600 MHz, DMSO-*d*₆) δ (ppm): 2.29 (s, 3H, CH₃), 5.18 (s, 2H, CH₂), 5.44 (s, 2H, CH₂), 6.95 (s, 2H, NH₂), 7.41 - 7.59 (m, 5H, Ar-H), 8.02 (s, 1H, CH), 8.19 (s, 1H, CH), 8.24 (s, 1H, CH); ¹³C NMR (100 MHz, DMSO-*d*₆) δ (ppm): 25.22, 46.74, 66.91, 108.45, 124.64, 126.94, 128.78, 130.03, 131.76, 143.22, 149.34, 156.16, 161.47, 167.11; MS (EI) (*m/z*, %): 323.4 (M⁺, 5.34); Elemental Analysis for C₁₆H₁₇N₇O (323.15): C, 59.43; H, 5.30; N, 30.32. Found: C, 59.65; H, 5.44; N, 30.24.

4.1.3.2 3-chlorobenzaldehyde *O*-((1-((4-amino-2-methylpyrimidin-5-yl) methyl)-1H-1, 2, 3-triazol-4-yl) methyl) oxime (4b**)**

Yellow solid; 0.33g; Yield 46 %; mp 154 - 155°C; ¹H NMR (DMSO-*d*₆, 600 MHz): δ 2.29 (s, 3H, CH₃), 5.21 (s, 2H, CH₂), 5.44 (s, 2H, CH₂), 6.94 (s, 2H, NH), 7.44 - 7.50 (m, 2H, Ar-H), 7.57 (d, 1H, J = 9.0 Hz, Ar-H), 7.65 (s, 2H, CH), 7.99 (s, 1H, CH), 8.20 (s, 1H, CH), 8.26 (s, 1H, CH); ¹³C NMR (DMSO-*d*₆, 100 MHz): δ 25.23, 46.83, 61.94, 100.68, 113.46, 116.36, 121.38, 124.96, 125.71, 133.81, 134.99, 135.80, 141.82, 156.38, 159.55, 161.53; MS (EI) (*m/z*, %): 357.2 (M⁺, 2.74); Elemental Analysis for C₁₆H₁₆ClN₇O (%): C, 53.71; H, 4.51; N, 27.40. Found: C, 53.51; H, 4.58; N, 27.69.

4.1.3.3 4-nitrobenzaldehyde *O*-((1-((4-amino-2-methylpyrimidin-5-yl) methyl)-1H-1, 2, 3-triazol-4-yl) methyl) oxime (4c**)**

Yellow solid; 0.48g; Yield 65 %; mp 214 - 216°C; ¹H NMR (DMSO-*d*₆, 600 MHz): δ 2.29 (s, 3H, CH₃), 5.26 (s, 2H, CH₂), 5.43 (s, 2H, CH₂), 6.96 (s, 2H, NH), 7.86 (d, 2H, J = 9.0 Hz, Ar-H), 8.22 (s, 1H, CH), 8.27 (d, 2H, J = 8.4 Hz, CH), 8.42 (s, 1H, CH); ¹³C NMR (DMSO-*d*₆, 100 MHz): δ 25.29, 46.78, 67.44, 124.02, 124.85, 127.92, 128.61, 138.05, 142.97, 147.95, 156.28, 161.43, 164.42, 167.42; MS (EI) (*m/z*, %): 368.1 (M⁺, 2.21); Elemental Analysis for C₁₆H₁₆N₈O₃ (%): C, 52.17; H, 4.38; N, 30.42. Found: C, 51.72; H, 4.23; N, 30.89.

4.1.3.4 4-chlorobenzaldehyde *O*-((1-((4-amino-2-methylpyrimidin-5-yl) methyl)-1H-1, 2, 3-triazol

-4-yl) methyl) oxime (4d)

Yellow solid; 0.56g; Yield 78 %; mp 185 - 187°C; ¹H NMR (DMSO-*d*₆, 600 MHz): δ 2.28 (s, 3H, CH₃), 5.18 (s, 2H, CH₂), 5.43 (s, 2H, CH₂), 6.94 (s, 2H, NH), 7.48 (d, 2H, *J* = 8.4 Hz, Ar-H), 7.61 (d, 2H, *J* = 8.4 Hz, Ar-H), 7.94 (s, 2H, CH), 8.19 (s, 1H, CH), 8.25 (s, 1H, CH); ¹³C NMR (DMSO-*d*₆, 100 MHz): δ 25.31, 46.97, 67.19, 125.00, 128.83, 129.16, 130.87, 134.89, 143.39, 148.63, 161.72, 162.77; MS (EI) (*m/z*, %): 357.3 (M⁺, 3.98); Elemental Analysis for C₁₆H₁₆ClN₇O (%): C, 53.71; H, 4.51; N, 27.40. Found: C, 53.32; H, 4.56; N, 27.02.

4.1.3.5 4-bromobenzaldehyde *O*-((1-((4-amino-2-methylpyrimidin-5-yl) methyl)-1H-1, 2, 3-triazol-4-yl) methyl) oxime (4e)

Yellow solid; 0.69g; Yield 86 %; mp 179 - 180°C; ¹H NMR (DMSO-*d*₆, 600 MHz): δ 2.31 (s, 3H, CH₃), 3.78 (s, 3H, CH₃), 5.15 (s, 2H, CH₂), 5.47 (s, 2H, CH₂), 6.98 (s, 2H, NH), 6.98 (s, 4H, Ar-H), 7.62 (d, 2H, *J* = 7.8 Hz, Ar-H), 7.94 (s, 1H, CH), 8.19 (s, 1H, CH), 8.24 (s, 1H, CH); ¹³C NMR (DMSO-*d*₆, 100 MHz): δ 25.29, 46.86, 67.11, 123.44, 124.81, 128.85, 131.08, 131.87, 143.25, 148.51, 156.11, 161.52, 162.44; MS (EI) (*m/z*, %): 403.3 (M⁺+2, 2.57), 401.2 (M⁺, 1.94); Elemental Analysis for C₁₆H₁₆BrN₇O (%): C, 47.44; H, 4.01; N, 24.37. Found: C, 46.95; H, 4.10; N, 24.21.

4.1.3.6 4-methoxybenzaldehyde *O*-((1-((4-amino-2-methylpyrimidin-5-yl) methyl)-1H-1, 2, 3-triazol-4-yl) methyl) oxime (4f)

Yellow solid; 0.21g; Yield 30 %, mp 100 - 101°C; ¹H NMR (DMSO-*d*₆, 600 MHz): δ 2.31 (s, 3H, CH₃), 3.78 (s, 3H, OCH₃), 5.15 (s, 2H, CH₂), 5.47 (s, 2H, CH₂), 6.98 (s, 4H, Ar+NH), 7.54 (s, 2H, Ar-H), 8.17 (s, 2H, CH); ¹³C NMR (DMSO-*d*₆, 100 MHz): δ 25.31, 36.09, 46.96, 67.19, 108.62, 125.00, 128.84, 129.16, 130.87, 134.89, 143.39, 148.63, 156.33, 161.72, 162.77; MS (EI) (*m/z*, %): 354.4 (M⁺+1, 1.37), 353.3 (M⁺, 6.40); Elemental Analysis for C₁₇H₁₉N₇O₂ (%): C, 57.78; H, 5.42; N, 27.75. Found: C, 57.30; H, 5.41; N, 27.56.

4.1.3.7 1-(3-chlorophenyl) ethanone *O*-((1-((4-amino-2-methylpyrimidin-5-yl) methyl)-1H-1, 2, 3-triazol-4-yl) methyl) oxime (4g)

Yellow solid; 0.47g; Yield 64 %; mp 131 - 133°C; ¹H NMR (DMSO-*d*₆, 600 MHz): δ 2.15 (s, 3H, CH₃), 2.29 (s, 3H, CH₃), 5.22 (s, 2H, CH₂), 5.44 (s, 2H, CH₂), 6.95 (s, 2H, NH), 7.42 - 7.48 (m, 2H,

Ar-H), 7.60 (d, 1H, $J = 7.2$ Hz, Ar-H), 7.67 (s, 1H, Ar-H), 8.00 (s, 1H, CH), 8.19 (s, 1H, CH); ^{13}C NMR (DMSO- d_6 , 100 MHz): δ 12.43, 25.25, 46.74, 67.08, 108.38, 108.30, 124.63, 125.59, 129.10, 130.32, 133.34, 137.91, 143.34, 153.69, 156.31, 161.49, 167.04; MS (EI) (m/z , %): 373.3 ($\text{M}^+ + 2$, 1.96), 371.3 (M^+ , 8.28); Elemental Analysis for $\text{C}_{17}\text{H}_{18}\text{ClN}_7\text{O}$ (%): C, 54.91; H, 4.88; N, 26.37. Found: C, 54.48; H, 4.62; N, 26.26.

4.1.3.8 1-(4-nitrophenyl) ethanone *O*-((1-((4-amino-2-methylpyrimidin-5-yl) methyl)-1H-1, 2, 3-triazol-4-yl) methyl) oxime (4h)

Yellow solid; 0.46g; yield 60 %; mp 222 - 224°C; ^1H NMR (DMSO- d_6 , 600 MHz): δ 2.21 (s, 3H, CH_3), 2.30 (s, 3H, CH_3), 5.27 (s, 2H, CH_2), 5.47 (s, 2H, CH_2), 6.98 (s, 2H, NH), 7.89 (s, 2H, Ar-H), 8.21 (s, 1H, CH), 8.25 (d, 2H, $J = 7.2$ Hz, Ar-H); ^{13}C NMR (DMSO- d_6 , 100 MHz): δ 11.87, 24.83, 46.27, 66.81, 108.68, 123.11, 124.31, 126.56, 141.35, 142.76, 147.15, 152.98, 155.63, 160.98, 167.12; MS (EI) (m/z , %): 383.3 ($\text{M}^+ + 1$, 1.28), 382.3 (M^+ , 8.05); Elemental Analysis for $\text{C}_{17}\text{H}_{18}\text{N}_8\text{O}_3$ (%): C, 53.40; H, 4.74; N, 29.30. Found: C, 53.61; H, 4.31; N, 29.12.

4.1.3.9 1-(4-chlorophenyl) ethanone *O*-((1-((4-amino-2-methylpyrimidin-5-yl) methyl)-1H-1, 2, 3-triazol-4-yl) methyl) oxime (4i)

Yellow solid; 0.67g; yield 90 %; mp 184 - 186°C; ^1H NMR (DMSO- d_6 , 600 MHz): δ 2.14 (s, 3H, CH_3), 2.29 (s, 3H, CH_3), 5.20 (s, 2H, CH_2), 5.44 (s, 2H, CH_2), 6.98 (s, 2H, NH), 7.47 (s, 2H, Ar-H), 7.64 (s, 2H, Ar-H), 8.19 (s, 1H, CH); ^{13}C NMR (DMSO- d_6 , 100 MHz): δ 12.25, 25.50, 46.74, 66.91, 122.69, 124.68, 127.85, 130.06, 131.31, 134.88, 143.51, 153.80, 155.72, 161.31, 168.79; MS (EI) (m/z , %): 373.2 ($\text{M}^+ + 2$, 2.06), 371.3 (M^+ , 7.27); Elemental Analysis for $\text{C}_{17}\text{H}_{18}\text{ClN}_7\text{O}$ (%): C, 54.91; H, 4.88; N, 26.37. Found: C, 54.45; H, 4.75; N, 26.18.

4.1.3.10 1-(4-bromophenyl) ethanone *O*-((1-((4-amino-2-methylpyrimidin-5-yl) methyl) -1H -1, 2, 3- triazol-4-yl) methyl) oxime (4j)

Yellow solid; 0.56g; Yield 66 %; mp 180 - 183°C; ^1H NMR (DMSO- d_6 , 600 MHz): δ 2.13 (s, 3H, CH_3), 2.30 (s, 3H, CH_3), 5.20 (s, 2H, CH_2), 5.49 (s, 2H, CH_2), 7.02 (s, 2H, NH), 7.57 (d, 2H, $J = 7.2$ Hz, Ar-H), 7.60 (d, 2H, $J = 7.8$ Hz, Ar-H), 8.19 (s, 1H, CH); ^{13}C NMR (DMSO- d_6 , 100 MHz): δ 12.25, 25.50, 46.74, 66.91, 122.69, 124.68, 127.85, 130.06, 131.31, 134.88, 143.51, 153.80, 155.72, 161.31,

168.79; MS (EI) (m/z , %): 417.2 (M^{+2} , 5.79), 415.2 (M^{+} , 6.78); Elemental Analysis for $C_{17}H_{18}BrN_7O$ (%): C, 49.05; H, 4.36; N, 23.55. Found: C, 49.23; H, 4.54; N, 23.91.

4.1.3.11 1-(4-methoxyphenyl) ethanone *O*-((1-((4-amino-2-methylpyrimidin-5-yl) methyl)-1H-1, 2, 3-triazol-4-yl) methyl) oxime (4k)

Yellow solid; 0.47g; Yield 64 %; mp 154 - 156°C; 1H NMR (DMSO- d_6 , 600 MHz): δ 2.12 (s, 3H, CH₃), 2.29 (s, 3H, CH₃), 3.77 (s, 3H, OCH₃), 5.16 (s, 2H, CH₂), 5.43 (s, 2H, CH₂), 6.95 (d, 4H, J = 9.0 Hz, Ar-H + NH), 7.58 (d, 2H, J = 9.0 Hz, Ar-H), 8.01 (s, 1H, CH), 8.17 (s, 1H, CH); ^{13}C NMR (DMSO- d_6 , 100 MHz): δ 12.43, 25.22, 46.69, 55.19, 66.71, 108.40, 113.81, 124.54, 127.37, 128.22, 143.64, 154.21, 156.28, 160.17, 161.51, 167.09; MS (EI) (m/z , %): 367.4 (M^{+} , 10.04); Elemental Analysis for $C_{18}H_{21}N_7O$ (%): C, 58.84; H, 5.76; N, 26.69. Found: C, 58.58; H, 5.62; N, 26.13.

4.1.3.12 1-(2-chlorophenyl) ethanone *O*-((1-((4-amino-2-methylpyrimidin-5-yl) methyl)-1H-1, 2, 3-triazol-4-yl) methyl) oxime (4l)

Yellow solid, 0.49g; Yield 67 %; mp 180 - 182°C; 1H NMR (DMSO- d_6 , 600 MHz): δ 2.14 (s, 3H, CH₃), 2.29 (s, 3H, CH₃), 5.20 (s, 2H, CH₂), 5.45 (s, 2H, CH₂), 6.98 (s, 2H, NH), 7.46 (s, 2H, Ar-H), 7.64 (s, 2H, Ar-H), 8.19 (s, 1H, CH); ^{13}C NMR (DMSO- d_6 , 100 MHz): δ 12.35, 25.22, 46.73, 66.94, 109.30, 124.63, 127.67, 128.46, 134.01, 134.60, 143.46, 153.76, 155.94, 158.09, 161.45, 167.35; MS (EI) (m/z , %): 373.3 (M^{+2} , 2.78), 371.3 (M^{+} , 7.22); Elemental Analysis for $C_{17}H_{18}ClN_7O$ (%): C, 54.91; H, 4.88; N, 26.37. Found: C, 54.18; H, 4.72; N, 26.46.

4.2 Structure-based docking

The crystallographic coordinates of the PDHc-E1 with ThDP from *E. coli* (PDB code: 1L8A) were obtained from the Brookhaven Data Bank for structure-based docking rational analyses. Hydrogen atoms were added to the structure allowing for appropriate ionization at physiological pH. The protonated state of several important residues such as His106, His142, Tyr177, Met194, Glu571, and His640 were adjusted with SYBYL7.3 (Tripos, St. Louis, MO, USA) to form hydrogen bonds with the ligand. Molecular docking analysis was performed with the SURFLEX module of SYBYL package to explore the interaction model for the active site of PDHc-E1 with its ligand especially with cofactor ThDP. All atoms located within 6.5 Å from any atom of the cofactor ThDP were selected into the

active site, and the corresponding amino acid residue was thus involved with the active site if only one of its atoms were selected. Other default parameters were adopted in the SURFLEX-docking calculations. All calculations were performed on the CCNU Grid website <http://www.202.114.32.71:8090/ccnu/chem/platform.xml>.

4.3 Inhibitory enzymatic activity evaluation and site-directed mutagenesis of PDHc E1

To evaluate the inhibitory activity of the compounds against PDHc E1, the half maximal inhibitory concentration (IC₅₀) values of the compounds were determined at the PDHc E1 enzyme level *in vitro*. The cloning, expression, purification and activity of PDHc E1 were carried out as described previously.¹⁸ ThDP and pyruvate were purchased from Sigma. Enzyme activities were measured as described previously.¹⁸ For IC₅₀ determination, we used a standard reaction mixture containing 50 mM K₃PO₄ (pH 6.4), 0.4 mM 2, 6-dichlorophenolindophenol (DCIP), 50 μM sodium pyruvate as substrate, 5 μg PDHc E1 purified enzyme and 50 μM ThDP. The compounds from 0 to 200 μM were incubated for 5 min with PDHc E1 at 37°C before the substrate (pyruvate) was added. The IC₅₀ values were determined by nonlinear least-squares fitting of the data using the Hill kinetic equations in Growth/sigmoidal model from origin 7.0 software as described previously.³⁰

Site-directed mutagenesis of PDHc E1 was accomplished by the introduction of specific base changes into a double-stranded DNA plasmid as described previously.³⁰ DNA encoding of the wild-type PDHc E1 cloned into the pMAL-C_{2x}-PDHc-E1 was used as a template for mutagenesis. The standard PCR mixture contained 50 - 100 ng of template DNA and 100 - 200 ng of each mutagenizing primer. The methylated plasmid was digested with DpnI, and 4 μL of each reaction was used to transform the DH5α competent cells. All mutations were confirmed by DNA sequencing. Verified plasmids containing the desired mutations were transformed into the *E. coli* TB1 strain. The mutant PDHc E1 proteins were purified in the same manner as the wild-type PDHc E1.

4.4 Inhibitory activity evaluation of compounds against against *Gibberella zeae* *in vivo*

Inhibitory activity evaluation of compounds **4h**, **4i**, and **4j** against *Gibberella zeae* *in vivo* were tested and their relative inhibitory ratio (%) had been determined by using the mycelium growth rate method³¹. Compound was dissolved in acetone. The solution was diluted in water to the required

concentration. The mycelial elongation (mm) of *Gibberella zeae* settlements was measured after 48 h of culture on potato glucose solid medium. The final concentration of the compound in medium was $100 \mu\text{g mL}^{-1}$. Three replicates of each test were carried out. The growth inhibition rates (I) were calculated with the equation: $I = [(C - T) / C] \times 100\%$, C is average diameter of mycelia in the presence of these compounds. The inhibition ratio of those compounds at the dose of $100 \mu\text{g mL}^{-1}$ was shown in **Table 1**.

4.5 Fluorescence spectral analyses

Fluorescence spectral analyses were carried out as described previously.³² All fluorescent measurements were carried out on a FluoreMax-P fluorescence spectrophotometer (HORIBA JOBIN YVON, France) equipped with a xenon lamp source and 1.0 cm quartz cell. The emission spectrum was recorded 305 - 500 nm range with excitation at 290 nm. The fluorescence quenching experiments of PDHc E1 or its mutants ($2 \mu\text{M}$) were performed at different concentrations of compounds by applying a 1-cm path length cuvette. The appropriate blank corresponding to the buffer was subtracted to correct the background of fluorescence. The binding constant (K) was calculated according to the equation: $\ln \frac{F_0 - F}{F} = \ln K + n \ln [Q]$, where F_0 and F are the fluorescence intensities without and with the ligand, respectively. Term $[Q]$ denotes the concentration of the quencher. A plot of $\ln [(F_0 - F)/F]$ vs. $\ln [Q]$ gave a straight line using least squares analysis. The Y-intercept was equal to $\ln K$ (K is equal to the binding constant).

Acknowledgments

This work was supported by the National Basic Research Program of China (No. 2010CB126100), the Natural Science Foundation of China (Nos. 21472061, 21373094, 21272089, 21172089, 21172090, 21072073, 20873049, 20872044, 30900054, and 30800169), the Program for New Century Excellent Talents in University (No. NCET-06-0673), the Program for Changjiang Scholars and Innovative Research Team in University (PCSIRT No. IRT0953), the Program for Academic Leader in Wuhan Municipality (No.201150530150), the Special Fund for Basic Scientific Research of Central Colleges

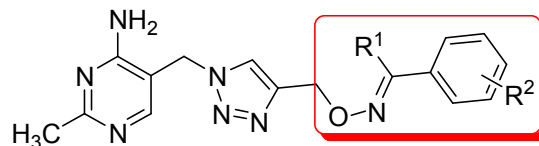
of Ministry of Education (Nos. CCNU09A01010, CCNU10C01002, and CCNU10A02006), and the Research Fund for the Doctoral Program of Higher Education of China (200805581146).

References

- 1 D. Ferná'ndez-Ortu'no, F. Chen and G. Schnabel, *Plant Dis.*, 2012, **96**, 1198
- 2 F. Qadri, A. M. Svennerholm, A. S. G. Faruque and R. B. Sack, *Clin. Microbiol. Rev.*, 2005, **18**, 465
- 3 H. Y. Sun, H. C. Wang, Y. Chen, H. X. Li, C. J. Chen and M. G. Zhou, *Plant Dis.*, 2010, **94**, 551
- 4 A. S. Puertoa, J. G. Fernandez, J. D. L. Castillob, M. J. S. Pinoa and G. P. Anguloa, *Diagn. Microbiol. Infect. Dis.*, 2006, **54**, 135
- 5 F. Jordan, N. Nemeria, F. Guo, I. Baburina, Y. Gao, A. Kahyaoglu, H. Li, J. Wang, J. Yi, J. R. Guest and W. Furey, *Biochim. Biophys. Acta (BBA)-Protein Struct. Mol. Enzymol.*, 1998, **1385**, 287
- 6 W. Wei, H. Li, N. Nemeria and F. Jordan, *Protein Expr. Purif.*, 2003, **28**, 140
- 7 R. H. Jackson and T. P. Singer, *J. Biol. Chem.*, 1983, **258**, 1857
- 8 A. Brown, N. Nemeria, J. Yi, D. Zhang, W. B. Jordan, R. S. Machado, J. R. Guest and F. Jordan, *Biochemistry*, 1997, **36**, 8071
- 9 E. Schoenbrunn-Hanebeck, B. Laber and N. Amrhein, *Biochemistry*, 1990, **29**, 4880
- 10 M. A. Apfel, B. H. Ikeda, D. C. Speckhard and P. A. Frey, *J. Biol. Chem.* 1984, **259**, 2905
- 11 J. A. Gutowski, G. E. Lienhard, *J. Biol. Chem.*, 1976, **251**, 2863
- 12 N. Nemeria, Y. Yan, Z. Zhang, A. M. Brown, P. Arjunan, W. Furey, J. R. Guest and F. Jordan, *J. Biol. Chem.*, 2001, **276**, 45969
- 13 K. Agyei-Owusu and F. J. Leeper, *FEBS J.*, 2009, **276**, 2905
- 14 P. Arjunan, N. Nemeria, A. Brunskill, K. Chandrasekhar, M. Sax, Y. Yan, F. Jordan, J. R. Guest and W. Furey, *Biochemistry*, 2002, **41**, 5213
- 15 P. Arjunan, K. Chandrasekhar, M. Sax, A. Brunskill, N. Nemeria, J. F. Frank and W. Furey, *Biochemistry*, 2004, **43**, 2405
- 16 H. W. He, J. L. Yuan, H. Peng, , T. Chen, , P. Shen, , S. Q. Wan, Y. J. Li, H. L. Tan, Y. H. He, J. B. He and Y. Li, *J. Agric. Food Chem.*, 2011, **59**, 4801

- 17 H. W. He, H. Peng, T. Wang, C. B. Wang, J. L. Yuan, T. Chen, J. B. He and X. S. Tan, *J. Agric. Food Chem.*, 2013, **61**, 2479
- 18 Y. L. Ren, J. B. He, L. L. Feng, X. Liao, J. Jin, Y. J. Li, Y. Cao, J. Wan and H. W. He, *Bioorg. Med. Chem.* 2011, **19**, 7501
- 19 K. Pericherla, P. Khedar, B. M. Khungar and A. Kumar, *Tetrahedron Lett.*, 2012, **53**, 6761
- 20 K. Slamova, P. Marhol, K. Bezouska, L. Lindkvist, S. Hansen, V. Kren and H. H. Jensen, *Bioorg. Med. Chem. Lett.*, 2010, **20**, 4263
- 21 S. Emami, M. Falahati, A. Banifatemi and A. Shafiee, *Bioorg. Med. Chem.*, 2004, **12**, 5881
- 22 A. Rossello, S. Bertini, A. Lapucci, M. Macchia, A. Martinelli, S. Rapposelli, E. Herreros and B. Macchia, *J. Med. Chem.*, 2002, **45**, 4903
- 23 H. J. Park, K. Lee, S. J. Park, B. Ahn, J. C. Lee, H. Y. Cho and K. I. Lee, *Bioorg. Med. Chem. Lett.*, 2005, **15**, 3307
- 24 C. Ramalingan, Y. T. Park and S. Kabilan, *Eur. J. Med. Chem.*, 2006, **41**, 683
- 25 J. T. Li, Y. X. Chen, X. L. Li and H. J. Deng, *Asian J. Chem.*, 2007, **19**, 2236
- 26 M. M. Pakulski, S. K. Mahato, M. J. Bosiak, M. P. Krzeminski and M. Zaidlewicz, *Tetrahedron: Asymmetry*, 2012, **23**, 716
- 27 K. M. Erixon, C. L. Dabalos and F. J. Leeper, *Org. Biomol. Chem.*, 2008, **6**, 3561
- 28 M. Meldal and C.W. Tornøe, *Chem. Rev.*, 2008, **108**, 2592
- 29 F. Jordan, Z. Zhang and E. Sergienko, *Bioorg. Chem.*, 2002, **30**, 188
- 30 L. L. Feng, Y. Sun, H. Deng, D. Li, J. Wan, X. F. Wang, W. W. Wang, X. Liao, Y. L. Ren and X. P. Hu, *FEBS J.*, 2014, **281**, 916
- 31 N. C. Chen, Bioassay of pesticides; Beijing Agricultural University Press: Beijing, China, 1991, pp 161-162
- 32 Y. Sun, X. Liao, D. Li, L. L. Feng, J. Li, X. F. Wang, J. Jin, F. Yi, L. Zhou and J. Wan, *Spectrochim. Acta A.*, 2012, **89**, 337

Table 1. Structures and inhibitory activities (IC_{50}) of novel thiamin diphosphate (ThDP) analog inhibitors (4a - 4l) against *E.coli* PDHc E1 and inhibition rate (%) of **4h**, **4i** and **4j** at $100 \mu\text{g ml}^{-1}$ against *Gibberella zeae*.



Number	Compd.	R ¹	R ²	IC ₅₀ (μM)	Inhibition rate (%)
1	4a	H	H	75.5 ± 0.02	N/A
2	4b	H	3-Cl	> 100	N/A
3	4c	H	4-NO ₂	17.8 ± 1.86	N/A
4	4d	H	4-Cl	59.4 ± 5.75	N/A
5	4e	H	4-Br	16.2 ± 1.76	N/A
6	4f	H	4-OCH ₃	31.4 ± 1.59	N/A
7	4g	CH ₃	3-Cl	57.8 ± 3.16	N/A
8	4h	CH ₃	4-NO ₂	6.7 ± 0.48	35
9	4i	CH ₃	4-Cl	6.9 ± 1.19	50
10	4j	CH ₃	4-Br	6.1 ± 0.48	33
11	4k	CH ₃	4-OCH ₃	30.2 ± 3.45	N/A
12	4l	CH ₃	2-Cl	14.9 ± 1.25	N/A

Scheme 1 Synthetic pathway of novel thiamin diphosphate (ThDP) **4a - 4l**. Reagents and conditions: (a) $\text{NH}_2\text{OH}\cdot\text{HCl}$, K_2CO_3 , EtOH, reflux, 7 h; (b) 3-Bromopropyne, NaOH, CH_3CN , reflux, 8 h; (c) NaN_3 , $\text{Na}_2\text{S}_2\text{O}_3$, H_2O , 60 - 65°C, 6 h; (d) **2a - 2l**, CuI, Et_3N , THF, rt, 10 - 15 h.

Fig.1 Structures of ThDP and the known potential ThDP analog inhibitors of PDHc E1.

Fig.2 Design of novel thiamin diphosphate (ThDP) inhibitors of PDHc E1.

Fig.3 Optimal binding model for compound **4j** into the active site of PDHc-E1 from *E.coli* docked by the SURFLEX module. The ligand and some key residues are presented as a stick model; hydrogen bonds are shown as dashed lines.

Fig. 4 The IC_{50} values of compound **4j** against the wild type (WT) and mutants of PDHc E1. The substrate is pyruvate acid, and the cofactor is ThDP.

Fig. 5 Binding constants (K_b) determined by fluorescence spectral analyses for the binding of compound **4j** to the wild type (WT) and mutants of PDHc E1

Scheme 1

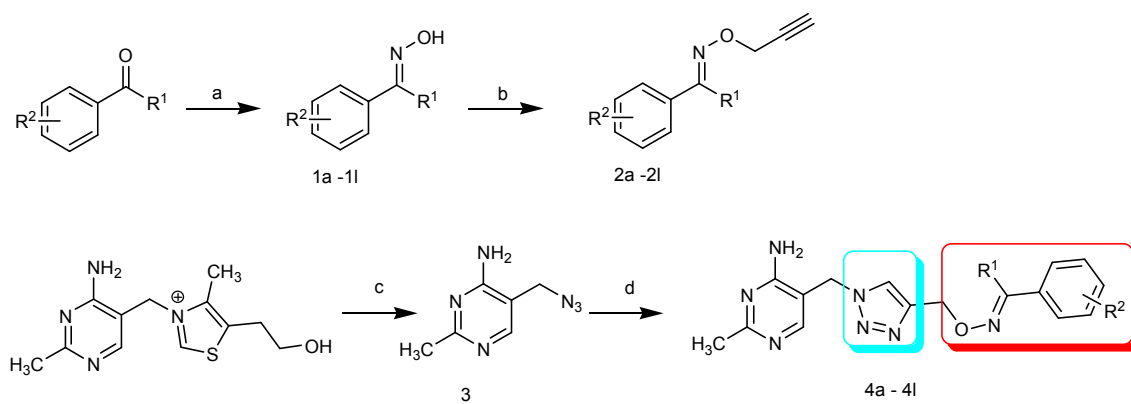
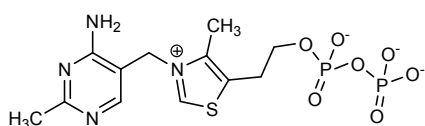
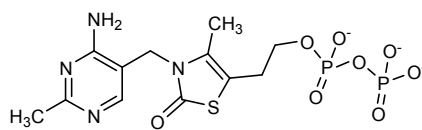


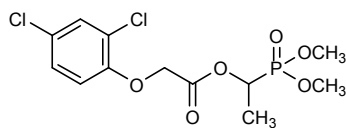
Fig.1



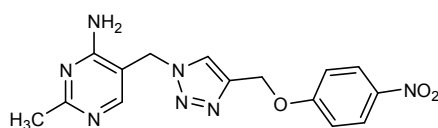
ThDP



ThTDP



HW02



Compound I

Fig. 2

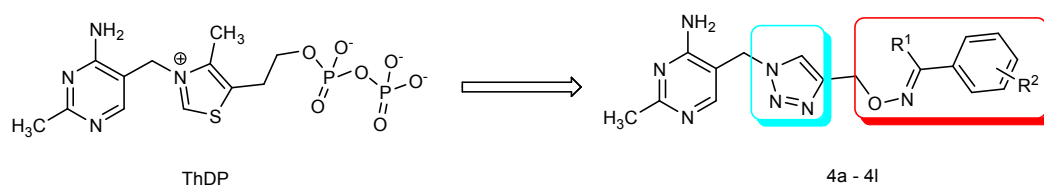


Fig. 3

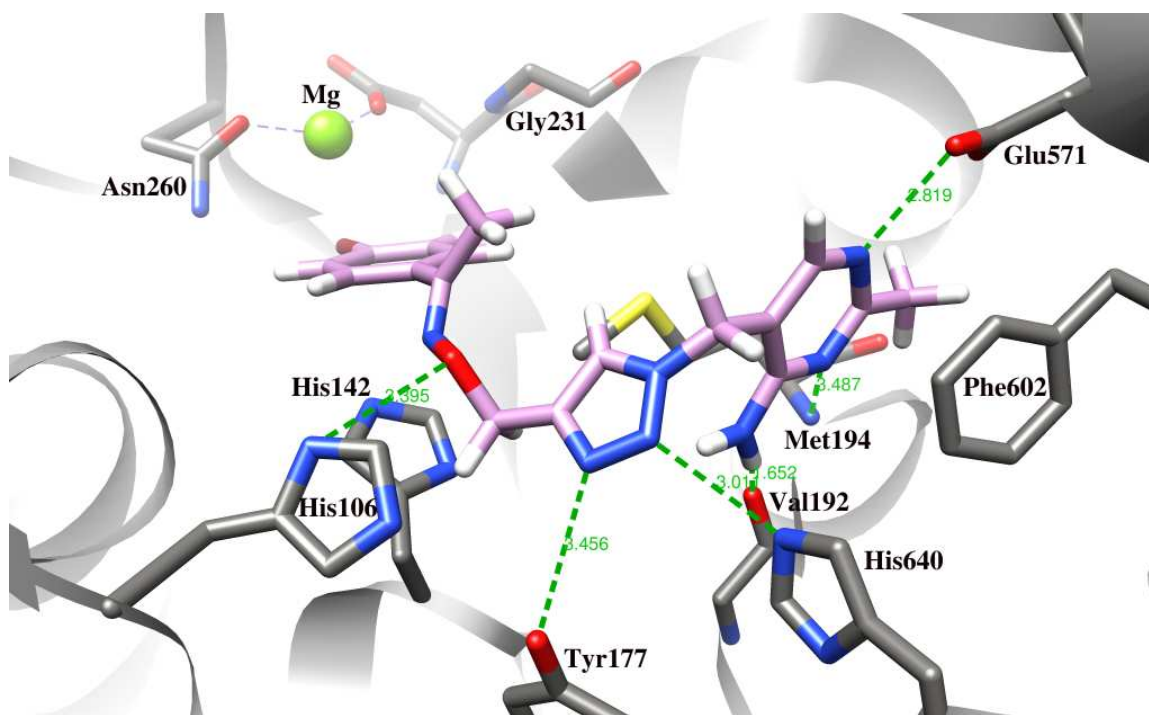


Fig. 4

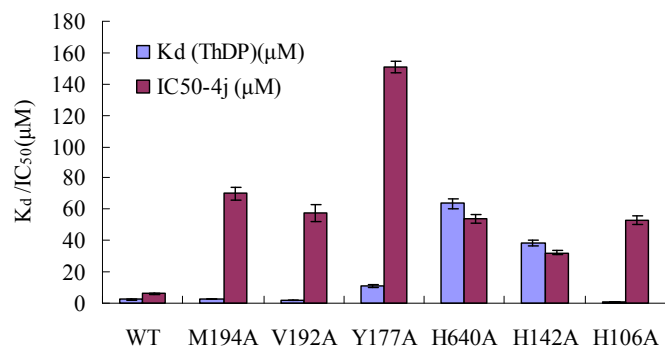


Fig. 5

